

Electronic Structures of Single-Walled Carbon Nanotubes Encapsulating Ellipsoidal C₇₀

Shingo Okubo,^{†,‡} Toshiya Okazaki,^{*,†,§} Kaori Hirose-Takai,[†] Kazu Suenaga,[†] Susumu Okada,^{||} Shunji Bandow,[⊥] and Sumio Iijima^{†,⊥}

National Institute of Advanced Industrial Science and Technology (AIST), Tsukuba 305-8565, Japan, PRESTO, Japan Science and Technology Agency (JST), 4-1-8 Honcho, Kawaguchi 332-0012, Japan, Institute of Physics and Center for Computational Sciences, University of Tsukuba, 1-1-1 Tennodai, Tsukuba 305-8577, Japan, CREST, Japan Science and Technology Agency, 4-1-8 Honcho, Kawaguchi 332-0012, Japan, and Department of Materials Science and Engineering, Meijo University, 1-501 Shiogamaguchi, Tenpaku-ku, Nagoya 468-8502, Japan

Received June 28, 2010; E-mail: toshi.okazaki@aist.go.jp

Abstract: The molecular orientation of ellipsoidal C₇₀ in single-walled carbon nanotubes (SWCNTs) depends on the tube diameter (d_t). Photoluminescence (PL) studies reveal that the fullerene encapsulation effects on the optical transition energy of SWCNTs are significantly different for C₇₀ and C₆₀ at $d_t = 1.405\text{--}1.431$ nm. This indicates that the transition from the “lying” alignment to the “standing” alignment occurs at $d_t \approx 1.41$ nm and the electronic states of SWCNTs are very sensitive to the interspacing between the encapsulated molecules and the SWCNTs. The present findings suggest that the electronic structure of SWCNTs is tunable not only by alternating the encapsulated molecules but also by controlling their molecular orientations, thus paving the way for development of novel SWCNT-based devices.

Introduction

Single-walled carbon nanotubes (SWCNTs) have attracted considerable attention for use as building blocks in future nanoelectronics because of their interesting electronic band structure that originates from their one-dimensional geometrical morphologies.¹ One of the basic approaches used for controlling the electronic structure is molecular doping. SWCNTs contain a hollow space inside the tube wall to accommodate doping materials. In fact, it is known that many molecules can be doped into the interior space, causing changes in the Fermi level and the band gap of the host SWCNTs.^{2–6} For example, scanning tunneling microscopy and spectroscopy (STM/STS) studies on SWCNTs encapsulating C₆₀ and Gd@C₈₂ (so-called “nanopeapods; NPDs”) revealed that the local density of states of

SWCNTs are modulated by fullerene encapsulation at the molecular level.^{7–9}

Recently, the mechanisms for modification of the electronic properties of SWCNTs employing molecular encapsulation have been investigated by photoluminescence (PL) and resonance Raman spectroscopy.^{10–15} These techniques can provide chirality-specific information regarding the produced NPDs, as in the case of empty SWCNTs. For C₆₀ encapsulation, the changes in the electronic structures were found to depend on the tube diameter.^{11–15} In the small-diameter regime ($1.25 < d_t < 1.32$ nm), the repulsive interaction is dominant because of the small interspacing between the C₆₀ cage and the tube wall ($l < 0.3$ nm). The repulsive interaction causes the radial expansion of the SWCNTs, which results in optical transition energy shifts

[†] National Institute of Advanced Industrial Science and Technology.
[‡] Current address: K. K. Air Liquide Laboratories, Tsukuba 300-4247, Japan.
[§] PRESTO, Japan Science and Technology Agency.
^{||} University of Tsukuba, 1-1-1 Tennodai, Tsukuba 305-8577, Japan, and CREST, Japan Science and Technology Agency.
[⊥] Meijo University.

(1) Avouris, P.; Chen, J. *Mater. Today* **2006**, *9*, 46–54.
(2) Monthieux, M. *Carbon* **2002**, *40*, 1809–1823.
(3) Okazaki, T.; Shinohara, H. In *Applied Physics of Nanotubes: Fundamentals of Theory, Optics and Transport Devices*; Rotkin, S. V., Subramoney, S., Eds.; Springer: Berlin, Germany, 2005; Chapter 5.
(4) Britz, D. A.; Khlobystov, A. N. *Chem. Soc. Rev.* **2006**, *35*, 637–659.
(5) Takenobu, T.; Takano, T.; Shiraiishi, M.; Murakami, Y.; Ata, M.; Kataura, H.; Achiba, Y.; Iwasa, Y. *Nat. Mater.* **2003**, *2*, 683–688.
(6) Shiozawa, H.; Rauf, H.; Pichler, T.; Knupfer, M.; Kalbac, M.; Yang, S.; Dunsch, L.; Büchner, B.; Kataura, H. *Phys. Rev. B* **2006**, *73*, 205411.

(7) Hornbaker, D. J.; Kahng, S.-J.; Misra, S.; Smith, B. W.; Johnson, A. T.; Mele, E. J.; Luzzi, D. E.; Yazdani, A. *Science* **2002**, *295*, 828–831.
(8) Lee, J.; Kim, H.; Kahng, S.-J.; Kim, G.; Son, Y.-W.; Ihm, J.; Kato, H.; Wang, Z. W.; Okazaki, T.; Shinohara, H.; Kuk, Y. *Nature* **2002**, *415*, 1005–1008.
(9) Cho, Y.; Han, S.; Kim, G.; Lee, H.; Ihm, J. *Phys. Rev. Lett.* **2003**, *90*, 106402.
(10) Li, L.-J.; Lin, T.-W.; Doig, J.; Mortimer, I. B.; Wiltshire, J. G.; Taylor, R. A.; Sloan, J.; Green, M. L. H.; Nicholas, R. J. *Phys. Rev. B* **2006**, *74*, 245418.
(11) Okazaki, T.; Okubo, S.; Nakanishi, T.; Joung, S.-K.; Saito, T.; Otani, M.; Okada, S.; Bandow, S.; Iijima, S. *J. Am. Chem. Soc.* **2008**, *130*, 4122–4128.
(12) Okubo, S.; Okazaki, T.; Kishi, N.; Joung, S.-K.; Nakanishi, T.; Okada, S.; Iijima, S. *J. Phys. Chem. C* **2009**, *113*, 571–575.
(13) Joung, S.-K.; Okazaki, T.; Kishi, N.; Okada, S.; Bandow, S.; Iijima, S. *Phys. Rev. Lett.* **2009**, *103*, 027403.
(14) Iizumi, Y.; Okazaki, T.; Liu, Z.; Suenaga, K.; Nakanishi, T.; Iijima, S.; Rotas, G.; Tagmatarchis, N. *Chem. Commun.* **2010**, *46*, 1293–1295.
(15) Joung, S.-K.; Okazaki, T.; Okada, S.; Iijima, S. *Phys. Chem. Chem. Phys.* **2010**, *12*, 8118–8122.

due to the strain effect. In the large-diameter regime ($d_t > 1.32$ nm), effective hybridization occurs between the electronic states of the C₆₀ and SWCNTs. The resultant attractive interaction between the SWCNTs and C₆₀ largely contributes to the optical transition energy changes in SWCNTs. It is interesting to note that the interaction is most effective at $l \approx 0.34$ nm ($d_t \approx 1.39$ nm), which is quite similar to the interlayer distance in graphite (0.335 nm).¹⁶

While C₆₀ can be regarded as a spherical “soccer ball” molecule, C₇₀ has an ellipsoidal “rugby ball” shape. Such ellipsoidal molecules are of particular interest because distinct orientations are possible for C₇₀ within the SWCNTs, which should lead to a unique modification of the electronic properties of the host SWCNTs. It has been reported that C₇₀ molecules can take two conformations inside SWCNTs, called “lying” and “standing” alignments, corresponding to the molecular long axis being parallel and perpendicular to the tube axis, respectively.^{17–23} Theoretical calculations predict that the electronic states of SWCNTs are sensitive to the orientation of the encapsulated C₇₀ molecules.²⁴ The difference in the interwall spacing of C₇₀ and SWCNTs results in the dependence of the electronic structures on the orientation. This implies that the electronic properties of SWCNTs can be tuned by controlling the orientation of the encapsulated C₇₀. However, there are limited experimental studies on the effects of C₇₀ encapsulation on the electronic states of SWCNTs. In this study, we carried out PL spectroscopy of C₇₀ NPDs over a wide diameter range ($d_t \approx 1.25–1.55$ nm). The results indicate that the electronic states of SWCNTs are very sensitive to the orientation of the encapsulated C₇₀, and C₇₀ change their orientations from the lying alignment to the standing alignment at $d_t \approx 1.41$ nm.

Experimental Section

Fullerenes C₆₀ and C₇₀ were generated by an arc-discharge method and purified by high-performance chromatography. We used two types of SWCNTs with different diameter distributions. One was synthesized by pulsed laser vaporization (PLV) of Ni–Co carbon target (diameter range 1.1–1.4 nm).²⁵ The other was synthesized by the arc discharge of a Ni–Y carbon rod (diameter 1.2–1.5 nm, APJ-A, purchased from Meijo Nano Carbon Co., Ltd.). The PLV- and arc-SWCNTs were purified according to the protocols reported by Kataura et al.¹⁸ and Okubo et al.,¹² respectively. For the preparation of NPDs, the purified PLV- or arc-SWCNTs were heated at 500 °C for 30 min to open the cap of the SWCNTs; they were then sealed with an excess amount of fullerene powder in a quartz tube under vacuum ($\sim 1 \times 10^{-4}$ Pa) and heated at 600 °C for 24 h. After the fullerene encapsulation, the remaining materials were washed with toluene and methanol several times and then dried under vacuum.

High-resolution transmission microscopy (HR-TEM) images were obtained using a JEOL JEM-2100F operated at 120 kV. For the HR-TEM observations, samples were dispersed in methanol by sonication (Ultrasonic Cleaner Vs-F100, operated at 100 W for a few minutes) and a small amount was taken from the samples in a glass Pasteur pipet with a bulb from which a tiny drop was deposited on a carbon-coated copper grid having 150 meshes.

For the PL measurement, a micelle solution of SWCNTs and NPD samples was prepared according to Bachilo et al.²⁶ The samples were dispersed in D₂O with 1 wt % sodium dodecylbenzene sulfonate (SDBS) by using a tip-type sonicator (Sonics VCX500, operated at 200 W for 10 min) and then centrifuged at 127 600g for 2.5 h. After centrifugation, the supernatant was collected for measurement. The PL measurement was performed using a Shimadzu NIR-PL system with an IR-enhanced InGaAs detector (Princeton Instruments OMA-V2.2) and a tunable Ti–sapphire laser (Spectra-Physics 3900S). The slit width for emission was 10 nm, and the scan steps were 5 and 2 nm for excitation and emission, respectively. The raw data, 1000–2200 nm for emission and 700–1060 nm for excitation, were corrected for wavelength-dependent factors and excitation laser intensities.

Results

TEM Observations. The encapsulation of the fullerenes into the SWCNTs was first confirmed by TEM observations, as shown in Figure 1. The TEM images clearly show that the C₇₀ fullerenes are tightly packed inside the SWCNTs (Figure 1A). Two different orientations of C₇₀ were observed, depending on the tube diameter.^{17–23} Though the lying alignment, in which the long axis of C₇₀ is parallel to the tube axis, was dominant in small-diameter tubes (Figure 1B), the standing alignment, where the short axis is parallel to the tube axis, was favored in large-diameter tubes (Figure 1C).

Photoluminescence Spectra. Figure 2 shows the PL map of C₇₀ NPDs with the reference spectra of the C₆₀ NPDs and SWCNTs, where PLV-SWCNTs were used as templates ($d_t = 1.2–1.4$ nm).¹¹ It is apparent that the PL pattern of the C₇₀ NPDs (Figure 2A) is completely different from that of the SWCNTs (Figure 2C) but very similar to that of the C₆₀ NPDs (Figure 2B). The PL peaks of C₆₀ NPDs have been determined by using more than 10 samples that have different chirality distributions and different filling yields.^{11,12} The peaks were reasonably consistent with the optical absorption and resonance Raman spectroscopy results.^{11–15} The similarity in the maps of C₇₀ NPDs and C₆₀ NPDs suggests that the PL peaks in the map of the C₇₀ NPDs can be assigned to each (n, m) tube as shown in Figure 2A,¹¹ where the PL peaks with identical $2n + m$ values are connected. Note that in Figure 2A and 2B we denoted solid circles only for the PL peaks originating from fullerene nanopeapods. Some SWCNTs such as the (11, 6) and (10, 8) tubes in the PLV-SWCNT samples have diameters that are too small to encapsulate fullerenes.¹¹ The PL peak positions of these SWCNTs actually remain unchanged after the doping processes (Figures 2A and 2B).¹¹

Even though the PL patterns of the C₇₀ NPDs and C₆₀ NPDs are similar, several differences can be observed between the two PL maps. For instance, while the PL peaks of (14, 3) C₆₀ NPDs ($d_t = 1.248$ nm) are observed in Figure 2B, the corresponding peak is absent in the case of the C₇₀ NPDs (Figure 2A). A diameter of 1.248 nm is the lower limit for C₆₀ encapsulation.^{11,13} The absence of the (14, 3) peak for the C₇₀ NPDs suggests that C₇₀ require larger interior space than C₆₀.

- (16) Palser, H. A. R. *Phys. Chem. Chem. Phys.* **1999**, *1*, 4459–4464.
- (17) Hirahara, K.; Bandow, S.; Suenaga, K.; Kato, H.; Okazaki, T.; Shinohara, H.; Iijima, S. *Phys. Rev. B* **2001**, *64*, 115420.
- (18) Kataura, H.; Maniwa, Y.; Abe, M.; Fujiwara, A.; Kodama, T.; Kikuchi, K.; Imahori, H.; Misaki, Y.; Suzuki, S.; Achiba, Y. *Appl. Phys. A: Mater. Sci. Process.* **2002**, *74*, 349–353.
- (19) Maniwa, Y.; Kataura, H.; Matsuda, K.; Okabe, Y. *New J. Phys.* **2003**, *5*, 127.
- (20) Khlbystov, A. N.; Scipioni, R.; Nguyen-Manh, D.; Britz, D. A.; Pettifor, D. G.; Briggs, G. A. D.; Lyapin, S. G.; Ardavan, A.; Nicholas, R. J. *Appl. Phys. Lett.* **2004**, *84*, 792–794.
- (21) Guan, L.; Li, H.; Shi, Z.; You, L.; Gu, Z. *Solid State Commun.* **2005**, *133*, 333–336.
- (22) Chorro, M.; Delhey, A.; Noe, L.; Monthieux, M.; Launois, P. *Phys. Rev. B* **2007**, *75*, 035416.
- (23) Verberck, B.; Michael, K. H. *Phys. Rev. B* **2007**, *75*, 045419.
- (24) Otani, M.; Okada, S.; Oshiyama, A. *Phys. Rev. B* **2003**, *68*, 125424.
- (25) Hirahara, K.; Suenaga, K.; Bandow, S.; Kato, H.; Okazaki, T.; Shinohara, H.; Iijima, S. *Phys. Rev. Lett.* **2000**, *85*, 5384–5386.

- (26) Bachilo, S. M.; Strano, M. S.; Kittrell, C.; Hauge, R. H.; Smalley, R. E.; Weisman, R. B. *Science* **2002**, *298*, 2361–2366.

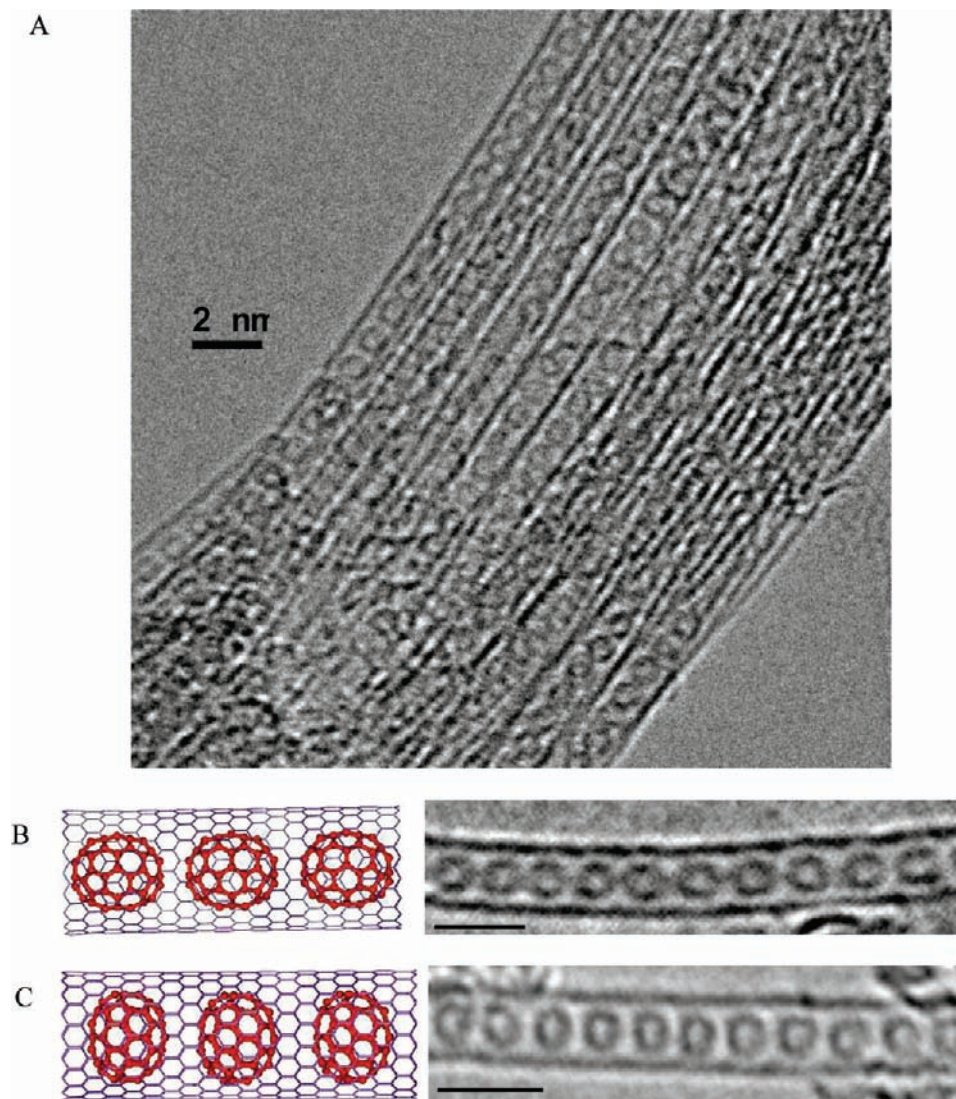


Figure 1. HRTEM image of (A) the bundled form of C_{70} NPDs and single C_{70} nanopeapods with (B) lying and (C) standing alignments. Scale bars = 2 nm.

In fact, as shown in Figure 2A, the PL peak positions change for SWCNTs with $d_t \geq 1.278$ nm ((13, 5) tubes), whereas those of SWCNTs with $d_t \leq 1.248$ nm were invariant. The observed values of the smallest diameters, i.e., 1.278 and 1.248 nm for C_{70} and C_{60} encapsulations, respectively, are in good agreement with the theoretically derived values, which are approximately 1.26 and 1.24 nm, respectively.^{22,24} Recent X-ray diffraction (XRD) experiments also corroborate the values of the difference in the threshold tube diameters for C_{70} and C_{60} encapsulations.²⁷ To reproduce the observed XRD spectra, tubes with a relatively large diameter are required for C_{70} encapsulations ($d_t > \sim 1.2$ nm) than for C_{60} encapsulations.²⁷

We also carried out the PL characterization of large-diameter C_{70} NPDs ($d_t = 1.3\text{--}1.55$ nm), where arc-SWCNTs were used as templates.¹² Figure 3A shows the PL map of arc-SWCNTs after C_{70} encapsulation along with the reference spectra of C_{60} NPDs (Figure 3B) and the original SWCNTs (Figure 3C). Again, the peak pattern of the C_{70} NPDs is quite similar to that

of the C_{60} NPDs. Hence, all the peaks of the C_{70} NPDs in the map can be mapped for each (n, m) tube by comparing them with the corresponding PL pattern of the C_{60} NPDs.¹² However, while the $2n + m$ family pattern exhibits a characteristic “hook” shape, the patterns are not smooth near the (14, 6) and (15, 5) tubes (Figure 3A). The observed emission and excitation energies (E_{11} and E_{22} , respectively) of the C_{70} NPDs are listed in Table 1.

Here we estimate the filling yields of molecular encapsulations from the observed PL intensities. To estimate the filling yields of C_{60} and C_{70} , the relative intensity of the PL peaks of (13, 5) NPDs and (13, 5) SWCNTs were calculated (Figures 2A, 2B, 3A, and 3B).²⁸ The PL peaks of (13, 5) NPDs do not overlap other peaks; this enables accurate yield estimations. The obtained values of relative intensity are 0.95 and 0.92 for PLV and arc C_{60} NPDs, respectively, and those for C_{70} NPDs are 0.77 and 0.74, respectively. Because the diameter of the (13, 5) tube is close to the lower limit for C_{70} encapsulation, the

(27) Launois, P.; Chorro, M.; Verberck, B.; Albouy, P.-A.; Rouzière, S.; Colson, D.; Forget, A.; Noé, L.; Karaura, H.; Monthieux, M.; Cambedouzou, J. *Carbon* **2010**, *48*, 89–98.

(28) In these calculations we assume that the PL intensity does not change after fullerene encapsulations. Because the encapsulated fullerenes may decrease the PL efficiency of SWCNTs, the estimated filling yields may be the lower limits of the true values.

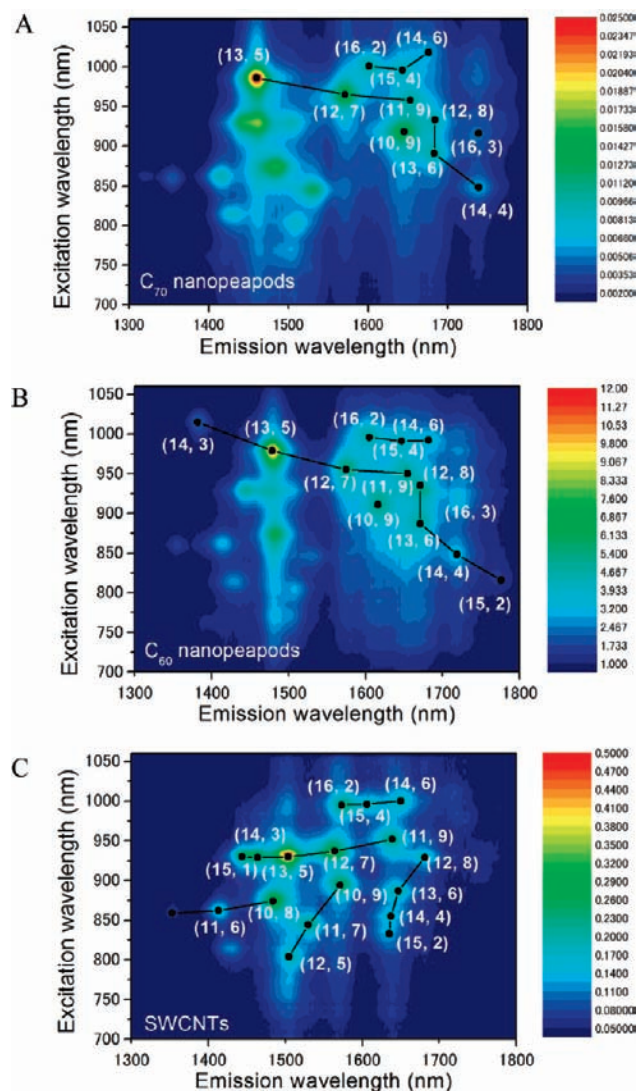


Figure 2. 2D PL contour plots of (A) C_{70} nanopeapods in SDBS– D_2O solutions along with reference spectra of (B) C_{60} nanopeapods and (C) PLV-SWCNTs.

relative PL intensity of (13, 5) C_{70} NPDs may be lower than that of C_{60} NPDs. A general impression obtained from the TEM observations is that the filling yield of the present C_{70} NPDs sample is comparable to that of the C_{60} NPDs.

Discussion

Mechanisms for Changing Optical Transition Energies in the Small-Diameter Regime ($d_t < \sim 1.32$ nm). We previously demonstrated that the optical transition energy of SWCNTs is substantially modified by C_{60} encapsulation, depending on the tube diameter.^{11,12} Figure 4A and 4B shows the energy differences in the values of E_{11} and E_{22} for the C_{60} NPDs and SWCNTs ($\Delta E_{ii} = E_{ii}^{NPDs} - E_{ii}^{SWCNTs}$, $i = 1, 2$) as a function of the tube diameter. Apparently, the diameter dependencies of ΔE_{11} and ΔE_{22} are different for type I ($\text{mod}(2n + m, 3) = 1$) and type II ($\text{mod}(2n + m, 3) = 2$) tubes. For example, ΔE_{11} for type I tubes has positive values in a relatively small-diameter regime ($d_t < \sim 1.32$ nm) (Figure 4A). With an increase in the tube diameter, it exponentially decreases to -0.02 eV and approaches zero. On the contrary, the negative ΔE_{11} for type II tubes increases to 0.02 eV with d_t and then gradually decreases again (Figure 4A). Similarly, ΔE_{22} clearly exhibits family-type

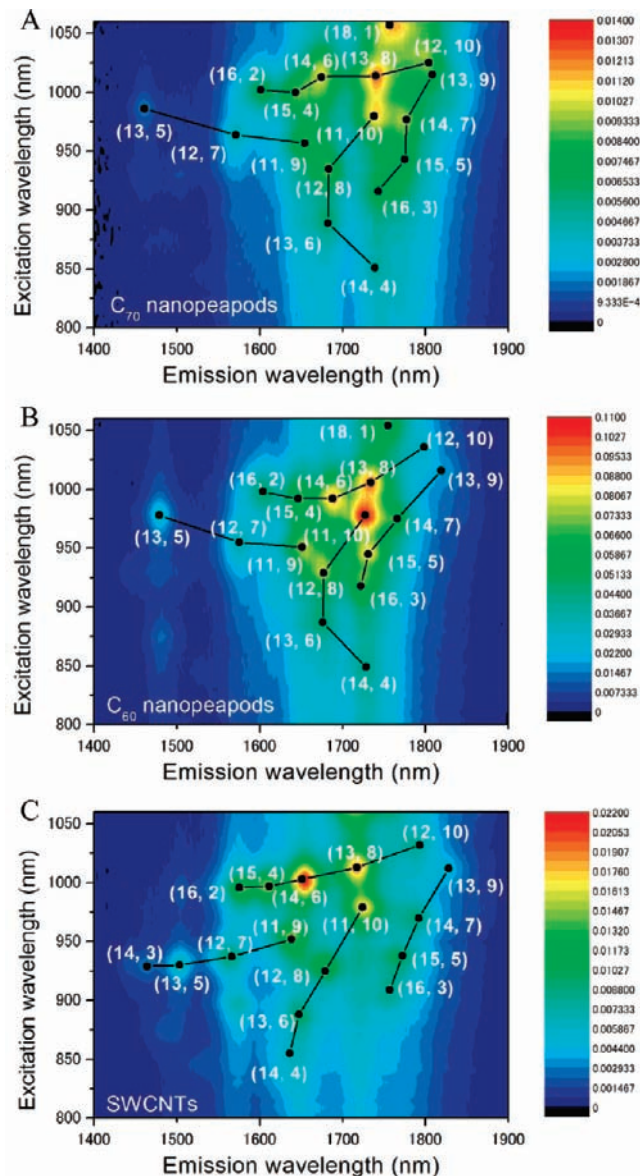


Figure 3. 2D PL contour plots of (A) C_{70} nanopeapods in SDBS– D_2O solutions along with reference spectra of (B) C_{60} nanopeapods and (C) arc-SWCNTs.

dependence (Figure 4B). That is, ΔE_{22} for type I tubes increases with the tube diameter and then decreases at $d_t \approx 1.4$ nm, whereas ΔE_{22} for type II tubes exhibits a totally opposite trend (Figure 4B). Such a strong dependence on the $2n + m$ family type is a characteristic feature of the strain-induced spectral shift.²⁹ In particular, the behaviors observed in the relatively small-diameter region ($d_t < \sim 1.32$ nm) can be attributed to the strain-induced energy shifts that result from the increase in the tube diameter due to the encapsulation of C_{60} .^{11,12}

Because the length of the short axis of C_{70} ($=0.712$ nm)³⁰ is similar to the diameter of C_{60} ($=0.710$ nm),³¹ C_{70} are expected to exhibit lying alignment in relatively small-diameter SWCNTs (Figure 1B), resulting in the enlargement of the tube diameter. Figure 4C and 4D shows the dependence of ΔE_{11} and ΔE_{22} on

(29) Yang, L.; Han, J. *Phys. Rev. Lett.* **2000**, *85*, 154–157.

(30) Nikolaev, A. V.; Dennis, T. J. S.; Prassides, K.; Soper, A. K. *Chem. Phys. Lett.* **1994**, *223*, 143–148.

(31) Johnson, R. D.; Bethune, D. S.; Yannoni, C. S. *Acc. Chem. Res.* **1992**, *25*, 169–175.

Table 1. Observed Optical Transition Energies of C₇₀ NPDs^a

(n, m)	d/nm	tube type	E ₁₁ /eV	E ₂₂ /eV
(13, 5)	1.278	I	0.849	1.258
(14, 4)	1.300	II	0.713	1.462
(10, 9)	1.307	II	0.754	1.351
(12, 7)	1.321	I	0.789	1.284
(13, 6)	1.336	II	0.737	1.391
(16, 2)	1.357	I	0.775	1.238
(11, 9)	1.377	I	0.750	1.295
(15, 4)	1.377	I	0.754	1.239
(12, 8)	1.384	II	0.736	1.329
(16, 3)	1.405	II	0.711	1.354
(14, 6)	1.411	I	0.741	1.223
(15, 5)	1.431	II	0.698	1.314
(11, 10)	1.444	II	0.713	1.259
(13, 8)	1.457	I	0.713	1.223
(14, 7)	1.470	II	0.698	1.270
(12, 10)	1.515	I	0.687	1.209
(13, 9)	1.521	II	0.686	1.222

^a Peak positions of each PL peak were obtained by curve fittings.

the diameter of the tube for C₇₀ NPDs. As observed in the case of C₆₀ NPDs, strong family-type dependence behaviors are also observed. For instance, ΔE₁₁ of the C₇₀ NPDs (type I) exhibits a positive value for (13, 5) tubes, becomes negative at around d_t ≈ 1.32 nm, and then approaches zero again (Figure 4C).

should be noted that for relatively small diameters (d_t < ~1.32 nm), ΔE₁₁ and ΔE₂₂ of the (13, 5) tube (type I) have opposite signs as opposed to those of the (14, 4) tube (type II) (Figure 4C and 4D). While this family-type dependence behavior can be explained by the radial expansion of SWCNTs upon C₇₀ encapsulation, the observed shifts are somewhat larger than those of (13, 5) and (14, 4) C₆₀ NPDs (Figure 4A and 4B).

The degree of radial expansion can be estimated by the following equation

$$\Delta E_{\text{gap}} = -\text{sgn}(2p + 1)3t_0(1 + \nu)\sigma \cos 3\theta \quad (1)$$

where p = mod(n-m, 3), t₀ (=2.66 eV) is the hopping parameter, ν (=0.2) is the Poisson's ratio, and σ is the radial expansion and/or tube compression.²⁹ For the (13, 5) tube (d_t = 1.278 nm), we observed shifts of 24 and 13 meV in the value of E₁₁ for C₇₀ and C₆₀ NPDs, respectively (Figure 4C and 4A); these values correspond to the radial expansion in the tube of 0.37% and 0.20%, respectively, according to eq 1. Hence, the difference in the tube diameter expansion (Δd_t) for C₇₀ and C₆₀ insertions can be calculated to be 0.0021 nm. The same analysis for the (14, 4) tube (d_t = 1.300 nm) results in a Δd_t = 0.0012 nm. Surprisingly, these values are almost identical with the difference between the length of the short axis of C₇₀ and the

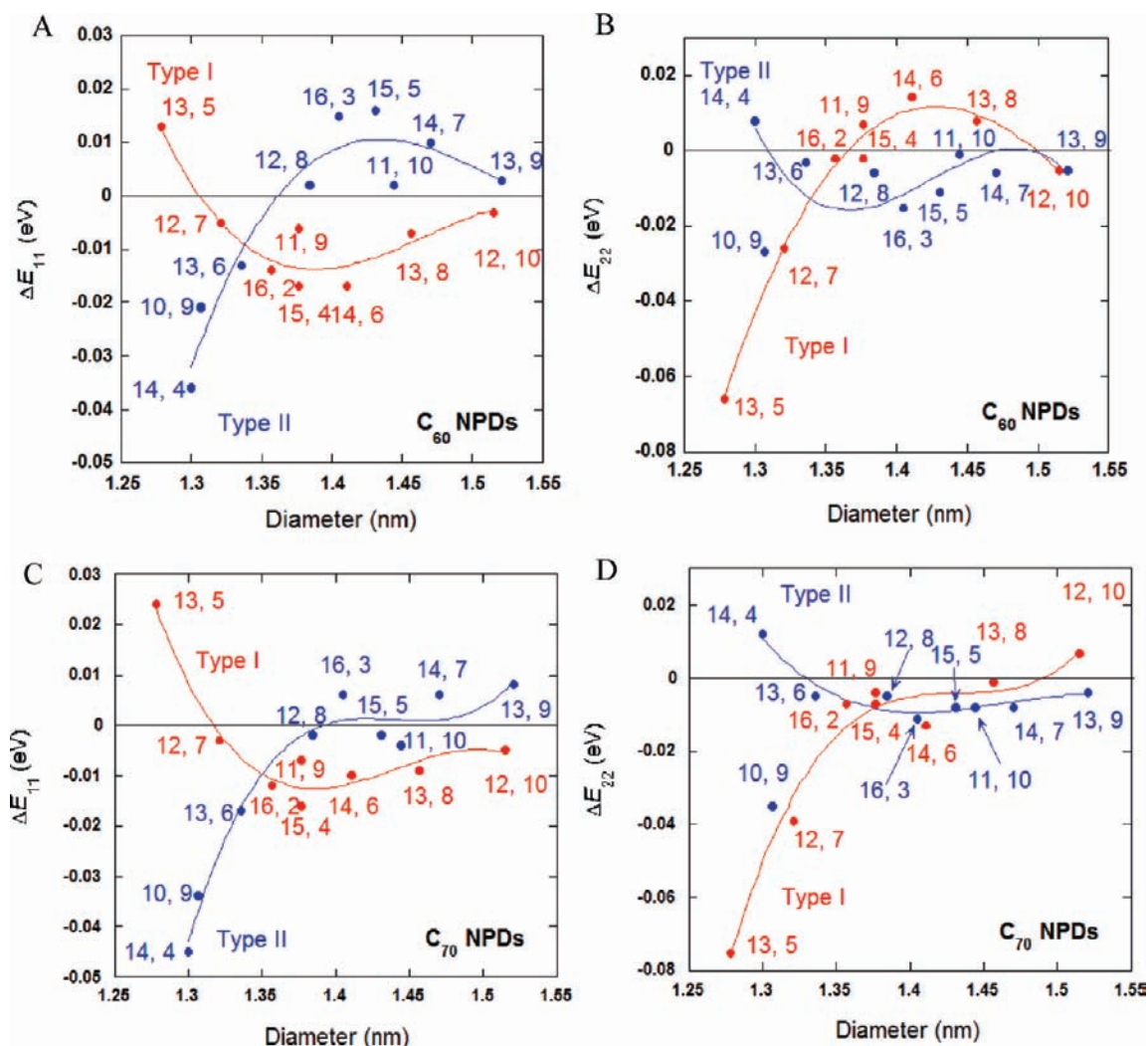


Figure 4. Differences in optical transition energies E₁₁ and E₂₂ (ΔE₁₁ and ΔE₂₂, respectively) for (A, B) C₆₀ NPDs and SWCNTs and those for (C, D) C₇₀ NPDs and SWCNTs as a function of tube diameter.

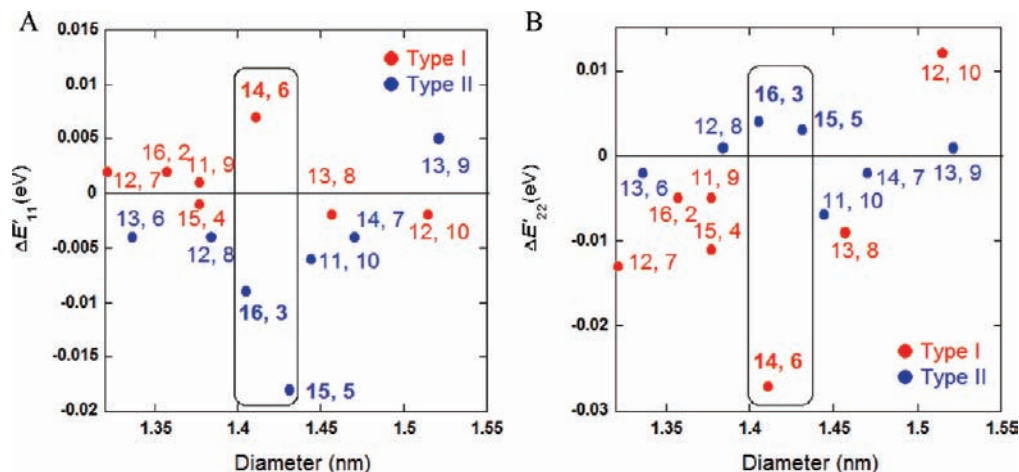


Figure 5. Differences between optical transition energies for (A) E_{11} and (B) E_{22} between C_{70} NPDs and C_{60} NPDs as a function of tube diameter ($d_t > 1.32$ nm).

diameter of C_{60} ($=0.002$ nm).^{30,31} SWCNTs can be used to detect such a minute difference in molecular size with a sensitivity of ~ 0.001 nm.

Mechanisms for Changing Optical Transition Energies in the Large-Diameter Regime ($d_t \sim 1.32$ nm). With an increase in the tube diameters, the local strain on the C_{60} encapsulation disappears^{11–13,15} and ΔE_{11} and ΔE_{22} approach zero (Figure 4A and 4B). Beyond the threshold diameter at $d_t \approx 1.32$ nm, the signs of ΔE_{11} and ΔE_{22} reverse (Figure 4A and 4B). In a relatively large-diameter regime such as this, the interaction between C_{60} and SWCNTs can be attributed to the hybridization between the π states of SWCNTs and those of C_{60} .^{11–13,15} The effective coupling between the electronic states has the same effect as the reduction in the effective tube diameter.¹² Such an attractive interaction is responsible for a negative ΔE_{11} and a positive ΔE_{22} for type I tubes, whereas the signs of ΔE_{11} and ΔE_{22} reverse for type II tubes, as observed in the diameter region (Figure 4A and 4B).^{11,12} In particular, the interaction is most effective at $d_t \approx 1.4$ nm (Figure 4A and 4B). Naturally, the interaction between C_{60} and SWCNTs becomes weaker when the distance between them increases.^{12,15} This tendency can be observed for diameters above 1.5 nm, where ΔE_{11} and ΔE_{22} approach the zero line (Figure 4A and 4B). It should be noted that according to theoretical calculations, the molecular arrangements of encapsulated C_{60} depend on the tube diameter.^{32,33} Hodak and Girifalco showed that C_{60} molecules are expected to adopt a zigzag structure at $d_t > 1.45$ nm.³² However, the present PL data suggest that C_{60} molecules may form linear chain arrangements until $d_t < 1.52$ nm because ΔE_{11} and ΔE_{22} monotonically approach zero lines.

On the other hand, ΔE_{11} and ΔE_{22} of the C_{70} NPDs exhibit analogous diameter dependence in this region (Figure 4C and 4D); however, the magnitude of the shifts becomes smaller than those of C_{60} NPDs. Figure 5 shows the differences in the values of E_{11} and E_{22} for the C_{70} and C_{60} NPDs ($\Delta E'_{ii} = E_{ii}^{C_{70}NPDs} - E_{ii}^{C_{60}NPDs}$, $i = 1, 2$) as a function of the tube diameter ($d_t > \sim 1.32$ nm). From the figure, it is clear that $\Delta E'_{11}$ and $\Delta E'_{22}$ of the (14, 6) (type I) and the (16, 3) and (15, 5) (type II) tubes ($d_t = 1.405$, 1.411, and 1.431 nm, respectively) are distinguishable from the other type I and type II tubes. (The characteristic behaviors of (12, 10) tubes will be discussed later).

The difference between the length of the long axis of C_{70} ($=0.796$ nm)³⁰ and the diameter of C_{60} ($=0.710$ nm)³⁰ is 0.086 nm. Previous studies that used PL patterns and Raman spectroscopy suggest that the smallest tube diameter for encapsulating C_{60} without friction is ~ 1.32 nm.^{11–13,15} Thus, if the tube diameter is more than ~ 1.406 nm, C_{70} molecules can find enough space to “stand up” inside SWCNTs. Surprisingly, the diameter of 1.406 nm is almost identical to that of the (16, 3) tubes (Table 1). This remarkable agreement strongly suggests that C_{70} molecules start to change their alignments in the (16, 3) tubes, which causes the optical transition energy changes observed here. Note that this transition diameter value is in good agreement with the previously reported values of 1.42 and 1.435 nm, which were estimated by XRD experiments and theoretical calculations, respectively.^{22,23}

The standing alignment of C_{70} results in an interspacing between C_{70} and the tube wall, which is substantially smaller than that of the C_{60} NPDs. As a result of the decrease in the interspacing, the interaction between C_{70} and SWCNTs becomes less attractive. The lower interaction between C_{70} and the SWCNTs should result in smaller spectral shifts. Notably, the values of ΔE_{11} and ΔE_{22} of the (16, 3), (14, 6), and (15, 5) C_{70} NPDs shift toward the zero line as compared to those of C_{60} NPDs (Figure 4).

Beyond the transition diameter, the standing C_{70} are energetically favorable.²⁴ Consequently, the attractive interaction between C_{70} and the SWCNTs occurs at $d_t \approx 1.5$ nm because the difference between the length of the long axis of C_{70} and the diameter of C_{60} is 0.086 nm.^{30,31} This type of attractive interaction should cause a large shift in E_{11} and E_{22} . The ΔE_{11} and ΔE_{22} values of the (12, 10) and (13, 9) C_{70} NPDs are consistent with this supposition (Figure 4). For instance, the ΔE_{11} and ΔE_{22} values of the (12, 10) C_{70} NPDs are smaller and larger than those of the (12, 10) C_{60} NPDs, respectively, presumably because of the more attractive interaction between C_{70} and the SWCNTs than that between C_{60} and the SWCNTs (Figure 4). The large $\Delta E'_{22}$ of (12, 10) tubes can also be explained by this mechanism (Figure 5).

The present findings suggest that the electronic properties of SWCNTs are tunable not only by alternating the encapsulated molecules but also by controlling their molecular orientations. Recent XRD experiments suggest that the dynamics of the encapsulated C_{70} depend on the ambient temperature.²⁷ The

(32) Hodak, M.; Girifalco, L. A. *Phys. Rev. B* **2003**, *67*, 075419.

(33) Okada, S.; Otani, M.; Oshiyama, A. *Phys. Rev. B* **2003**, *67*, 205411.

standing C_{70} molecules start to rotate at a high temperature (from ~ 373 K).²⁷ A transition from standing to rotating molecules should cause the change in the interaction between SWCNTs and C_{70} , leading to modification of the electronic structure of the SWCNTs. A sudden heating of the C_{70} NPDs, for example, by photoexcitation, is effective for controlling the molecular orientation of C_{70} .

The control of the electronic properties of SWCNTs by manipulating the orientation of the encapsulated molecules has several intrinsic advantages. First, the process does not destroy the chemical bonds in the tube wall, thus completely preserving the superior properties of SWCNTs. Because the encapsulated molecules are blocked from active species such as oxygen, these elements are expected to be robust and reversible. Furthermore, SWCNT heterostructures, where different sections of a single SWCNT have different bandgaps, can be created in a controllable manner by changing the molecular orientation of the encapsulated molecules.

Conclusion

We investigated the effect of C_{70} encapsulation on the electronic structure of SWCNTs over a wide tube diameter range ($d_t \approx 1.25$ – 1.55 nm). The obtained PL peak shifts clearly indicate that the changes in the electronic states of SWCNTs are related to the interspacing between the encapsulated molecules and the tube wall. This implies that it is possible to tune the electronic properties of SWCNTs by controlling the orientation of the encapsulated molecules, thereby paving the way for the design of CNT-based organic electronics.

Acknowledgment. We thank R. Takano (AIST) for her assistance with the experiments. T.O. acknowledges the Grant-in-Aid received from MEXT, Japan (no. 21685017). Part of this work was supported by the NEDO Nano-Carbon Technology project.

JA105654G